



Since January 2020 Elsevier has created a COVID-19 resource centre with free information in English and Mandarin on the novel coronavirus COVID-19. The COVID-19 resource centre is hosted on Elsevier Connect, the company's public news and information website.

Elsevier hereby grants permission to make all its COVID-19-related research that is available on the COVID-19 resource centre - including this research content - immediately available in PubMed Central and other publicly funded repositories, such as the WHO COVID database with rights for unrestricted research re-use and analyses in any form or by any means with acknowledgement of the original source. These permissions are granted for free by Elsevier for as long as the COVID-19 resource centre remains active.



Contents lists available at ScienceDirect

International Journal of Biochemistry and Cell Biology

journal homepage: www.elsevier.com/locate/biocel

Identification and application of self-binding zipper-like sequences in SARS-CoV spike protein

Si Min Zhang^{a,b}, Ying Liao^c, Tuan Ling Neo^a, Yanning Lu^a, Ding Xiang Liu^a, Anders Vahlne^b, James P. Tam^{a,*}

^a School of Biological Sciences, Nanyang Technological University, Singapore

^b Division of Clinical Microbiology, Department of Laboratory Medicine, Karolinska Institutet, Sweden

^c Shanghai Veterinary Research Institute, Chinese Academy of Agricultural Sciences, Shanghai, China

ARTICLE INFO

Keywords:

Steric β -zipper
SARS-CoV spike protein
Class I viral fusion glycoprotein
self-binding peptides
viral detection

ABSTRACT

Self-binding peptides containing zipper-like sequences, such as the Leu/Ile zipper sequence within the coiled coil regions of proteins and the cross- β spine steric zippers within the amyloid-like fibrils, could bind to the protein-of-origin through homophilic sequence-specific zipper motifs. These self-binding sequences represent opportunities for the development of biochemical tools and/or therapeutics. Here, we report on the identification of a putative self-binding β -zipper-forming peptide within the severe acute respiratory syndrome-associated coronavirus spike (S) protein and its application in viral detection. Peptide array scanning of overlapping peptides covering the entire length of S protein identified 34 putative self-binding peptides of six clusters, five of which contained octapeptide core consensus sequences. The Cluster I consensus octapeptide sequence GINTNFR was predicted by the Eisenberg's 3D profile method to have high amyloid-like fibrillation potential through steric β -zipper formation. Peptide C6 containing the Cluster I consensus sequence was shown to oligomerize and form amyloid-like fibrils. Taking advantage of this, C6 was further applied to detect the S protein expression *in vitro* by fluorescence staining. Meanwhile, the coiled-coil-forming Leu/Ile heptad repeat sequences within the S protein were under-represented during peptide array scanning, in agreement with that long peptide lengths were required to attain high helix-mediated interaction avidity. The data suggest that short β -zipper-like self-binding peptides within the S protein could be identified through combining the peptide scanning and predictive methods, and could be exploited as biochemical detection reagents for viral infection.

1. Introduction

Severe acute respiratory syndrome (SARS) is a contagious atypical pneumonia that caused an epidemic between November 2002 and July 2003 with a 9.6% mortality rate (8096 known cases and 774 deaths) (http://www.who.int/csr/sars/country/table2004_04_21/en/). While the SARS-CoV epidemic has subsided, the closely related Middle East respiratory syndrome coronavirus (MERS-CoV) infection is still presenting severe public health threats locally and globally. Generation of effective anti-viral therapeutic and detection agents is warranted, and the SARS-CoV spike (S) protein, which mediates viral entry and initiates viral infection, represents attractive drug development target. The SARS-CoV surface spike (S) glycoprotein is composed of the surface-exposed S1 subunit and the transmembrane S2 subunit which further

hetero-trimerize on the viral envelope, a characteristic structural prerequisite for Class I fusion glycoproteins to facilitate viral entry (Fig. 1) (Bosch et al., 2003; Xiao and Dimitrov, 2004). Specifically, following the recognition of the cellular receptor angiotensin-converting enzyme 2 (ACE2) by the receptor binding domain (RBD) within the surface S1 subunit, structural changes are induced within the S2 subunit, exposing the fusion peptide (FP) within S2 and enabling it to be inserted into the target cell membranes. This leads to the heptad repeat 1 (HR1) regions C-terminal to the FP to oligomerize in an antiparallel fashion with the more C-terminal HR2 regions of the S protein trimers, resulting in a coiled-coil structure, *i.e.*, the six-helix bundle (6-HB) fusion cores (Bosch et al., 2003). The 6-HB structure is further strengthened by hetero-dimerization of the hydrophobic regions flanking the two HRs, specifically the membrane proximal external region (MPER) and the S2

Abbreviations: S, Spike protein; HR, Heptad repeat; HIV-1, Human immunodeficiency virus type I; SARS-CoV, Severe acute respiratory syndrome associated coronavirus; RBD, Receptor binding domain; FP, Fusion peptide; 6-HB, Six-helix bundle; MPER, Membrane proximal external region; IFP, Internal fusion peptide; HA, Hemagglutinin; PAGE, Polyacrylamide gel electrophoresis; CD, Circular dichroism; ThT, Thioflavin T

* Corresponding author.

E-mail address: jptam@ntu.edu.sg (J.P. Tam).

<https://doi.org/10.1016/j.biocel.2018.05.012>

Received 7 December 2017; Received in revised form 3 May 2018; Accepted 21 May 2018

Available online 22 May 2018

1357-2725/© 2018 Elsevier Ltd. All rights reserved.

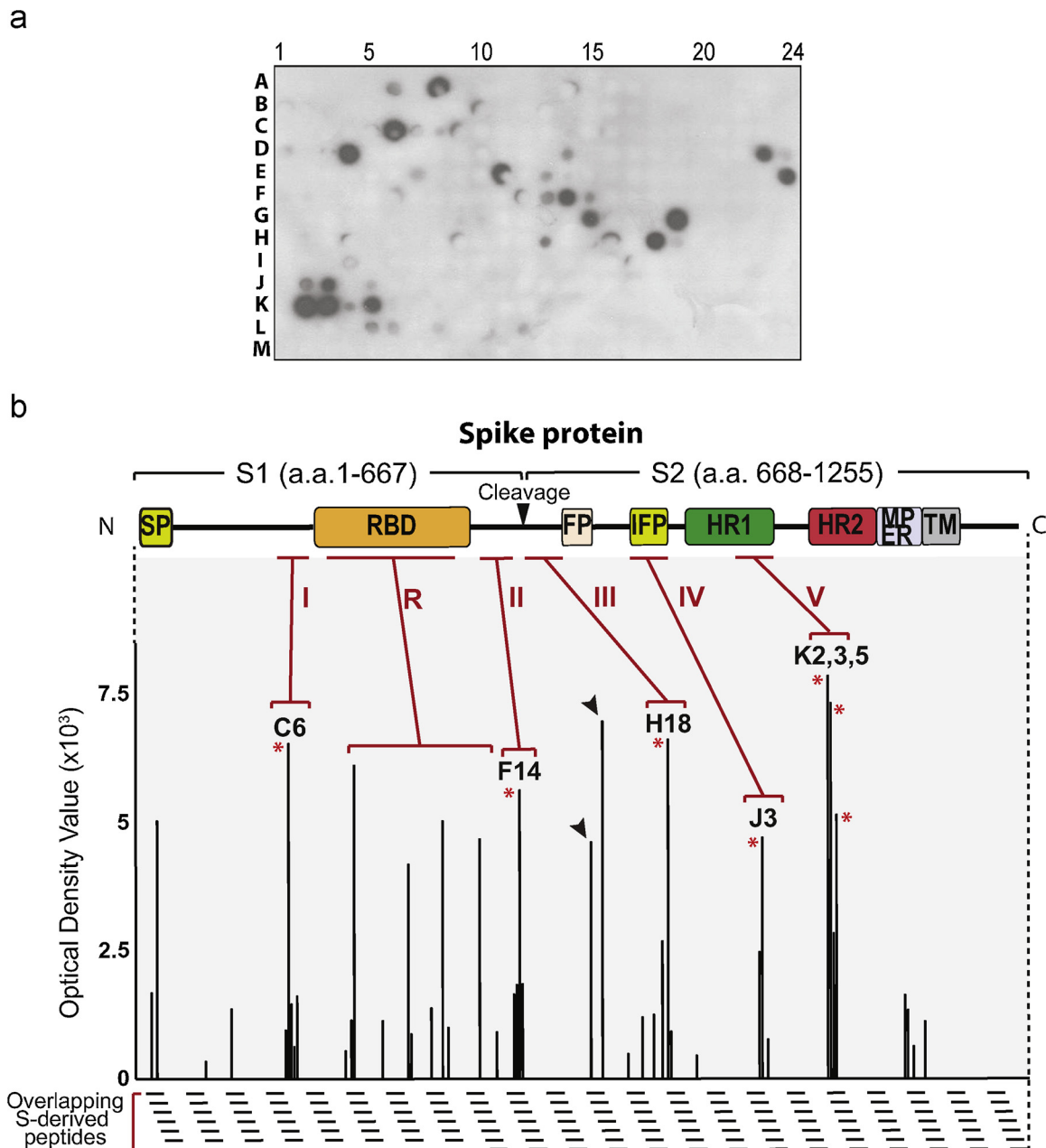


Fig. 1. Screening of the 20-residue peptide array library with S1188HA expressed in Sf9 cells. **a.** Screening result of the 20-residue peptide array library. Retained S1188HA was identified as dark spots on the peptide-spotted membrane. **b.** Densitometry analysis of the positive spots in A revealed the S1188HA-binding pattern. Five high-affinity-binding clusters (I, II, III, IV, and V), which contained three out of six consecutive peptides exhibiting optical density values at least 2.5 times of the background level (Rigter et al., 2007), were shown with the representative peptides (*). RBD-derived peptides bound to S1188HA with high affinity were clustered as Cluster R. False positive peptides that bound to the detection antibodies were indicated by the arrow heads and excluded in data analysis.

internal fusion peptide (IFP) (Guillen et al., 2008; Liao et al., 2015). Collectively, the opposing viral and cellular membranes are juxtaposed into proximity for the subsequent fusion and viral entry (Bosch et al., 2003).

One of the approaches to generate anti-viral therapeutics has been focused on self-binding peptides. Self-binding peptides bind to their cognate proteins through sequence-specific interactions (Beisswenger and Cabrele, 2014; Hard and Lendel, 2012), with examples including Leu/Ile zipper sequences in coiled-coil motifs (Hakoshima, 2001; Perutz, 1994), cross- β spine steric zipper sequences (abbreviated as steric β -zipper) in amyloid and amyloid-like fibrils (Nelson et al., 2005; Parry, 2005; Sawaya et al., 2007), and aromatic-residue-rich sequences in aromatic zippers (Cochran et al., 2001), among others. Their abilities to conduct sequence-specific interactions have been exploited and been

further developed into peptidyl therapeutics and biochemical reagents (Azzarito et al., 2013; Hakoshima, 2001). For anti-viral applications, Leu/Ile zipper-like sequences within HRs have successfully been developed as entry inhibitors against infections such as the human immunodeficiency virus type I and SARS-CoV (Borrego et al., 2013; Bosch et al., 2004; Liu et al., 2005, 2004; Medinas et al., 2002; Wang et al., 2011; Wild et al., 1994; Yao and Compans, 1996; Young et al., 1999). Specifically, the HR-derived Leu/Ile zipper-like peptides can bind to the fusion glycoprotein in a dominant-negative fashion, and thereby halt the viral entry and infection.

According to our understanding of the literature, aside from the Leu/Ile zipper-like sequences within S2 subunit, other potentially self-interacting zipper-like sequences in other S protein domains that mediate the multi-step viral entry process of SARS-CoV are less known

and studied. The globular S1 subunit is structurally different from S2 subunit, and is largely composed of β -sheets, such as within the RBD (Giannecchini et al., 2005). Logically, identification of zipper-like sequences within the S1 subunit should focus on β -zipper-like motifs, which include steric β -zippers. These complementary, dry, puzzle-like interfaces, form between as few as four and as many as seven tightly interdigitating side chains of two facing peptide β -sheets (Azriel and Gazit, 2001; Balbach et al., 2000; Balbirnie et al., 2001; Nelson et al., 2005; Reches et al., 2002; Tenidis et al., 2000; von Bergen et al., 2000). Self-binding peptides containing this motif have been shown to recognize and homo-dimerize with the same sequence within amyloid-like fibrils and then inhibit the fibrillation process (Hard and Lendel, 2012). This suggests that the steric beta-zipper sequences within a viral fusion glycoprotein, such as SARS-CoV S protein, could also bind to the cognate viral fusion protein through homophilic interaction, and could further serve as a biochemical reagent for viral detection and/or as antiviral therapeutics.

In the current study, we identified the self-binding β -zipper-like peptides within the S protein of SARS-CoV. Firstly, putative self-binding peptides were identified by screening a peptide array library that was composed of overlapping peptides covering the entire length of S protein (Kaukinen et al., 2003; Rigter et al., 2007; Uttamchandani and Yao, 2008). The identified peptides were further analyzed by the 3D profile method to predict the steric β -zipper segments. Subsequently, a peptide that potentially oligomerized through forming steric β -zippers was identified experimentally and further used to detect S protein expression *in vitro*. Finally, we could demonstrate the differential influences of peptide lengths on β - or helix-mediated interactions. Altogether, these data suggest that endogenous steric β -zipper peptides within viral fusion proteins, such as SARS-CoV S protein, could be a practical source for developing detection reagents against viral infections.

2. Materials and methods

2.1. Cell lines and plasmids

Plasmid pXJ40-S encoding the full-length S protein of SARS-CoV, S1255, (Sin 2774, accession number: P59594) was kindly provided by the Institute of Molecular Cell Biology, Singapore. Plasmid pcDNA3.1-OPTS-HA encoding a HA-tagged codon-optimized full-length S protein under a 5' T7 promoter was kindly provided by Dr. Zhang Linqi from the Aaron Diamond AIDS Research Center (Chen et al., 2005). Plasmid pVL1392(S1188HA) encoding the ectodomain (aa 1-1188) of the S protein (Sin 2774) with a C-terminal human influenza hemagglutinin (HA) tag was constructed from pXJ40-S (Lu et al., 2008a).

2.2. Peptide array library construction and Fmoc solid phase peptide synthesis

Peptide array libraries containing SARS-CoV (Sin 2774) S protein-derived overlapping peptides were synthesized and simultaneously anchored through the C-termini on PEG-derivatized membranes (Amino-PEG500 -UC540 Sheet, Intavis AG, Germany), using Fmoc chemistry and MultiPep (SPOT) synthesizer (Intavis AG, MultiPep, Germany) (Frank, 2002; Frank and Overwin, 1996). S protein-derived peptides were chemically synthesized with or without C-terminal biotin tags using 0.1 mM biotinylated Rink and Wang resins, respectively, using the Liberty-1™ automated microwave peptide synthesizer under the programed microwave conditions, using 4 equiv. Fmoc aa deprotected by 20% piperidine in dimethylformamide, 4 equiv. (benzotriazol-1-yloxy) tripyrrolidinophosphonium hexafluorophosphate and 6 equiv. N,N-diisopropylethylamine in dimethylformamide. The assembled peptide was subsequently de-protected with reagent R (15 ml of 90% TFA, 5% Thioanisole, 3% EDT, and 2% Anisole), precipitated with cold diethyl ether and finally purified by reversed-phase HPLC. Peptides were confirmed by MALDI-TOF mass spectrometry.

2.3. Peptide array screening and pull down experiments

Peptide array library on PEG-derivatized membranes or biotinylated peptides mixed with UltraLink® Immobilized NeutrAvidin™ resins (Pierce) were blocked with Superblock® Blocking Buffer (Pierce) and probed with S1188HA-containing Sf9 cell lysates (Lu et al., 2008a), at RT for 1 h in 200 μ L binding buffer (PBS, 1% NP40, 0.1% Sodium dodecyl sulfate (SDS), 2 M urea). S1188HA retained on the peptide array membrane or resin-bound peptides was detected via chemiluminescence immunoassay or Western blot, respectively, using rabbit anti-HA (Y-11) (Santa Cruz Biotechnology, USA) followed by HRP-conjugated swine anti-rabbit secondary antibody (Dako, Denmark).

2.4. Chemical crosslinking

Biotinylated peptides (1 mM) were incubated with 0, 1, 5, or 10 mM glutaraldehyde at RT for 1 h, followed by quenching with 100 mM glycine. Peptide oligomers were then separated on 16% Tricine SDS-PAGE and analyzed by Western blot using avidin-HRP (Santa Cruz Biotechnology, USA).

2.5. Prediction of the amyloid-like fibril-forming segments by the 3D profile method

Sequence of the SARS-CoV S protein (Sin 2774) was analyzed with the 3D profile method (available online at <http://services.mbi.ucla.edu/zipperdb/>) to predict amyloid-like sequences, with the cut-off ROSETTA energetic scores set at -3.7 kcal/mol/residue (Thompson et al., 2006).

2.6. Circular dichroism (CD) spectroscopy

CD spectroscopy analysis was performed as previously described (Zhang et al., 2015). Briefly, peptides dissolved in ddH₂O were measured by a Chirascan circular dichroism spectrometer (Applied Photophysics) between 180 nm and 260 nm, with a 0.5 nm step resolution. The secondary structure of the peptide was estimated as previously described (Zhang et al., 2015).

2.7. Congo Red and Thioflavin T (ThT) assays

Amyloid-like fibrils were identified through the Congo Red and ThT assays, as previously described (Nilsson, 2004). Briefly, following a three-day incubation in DMSO at 10 mg/ml, peptides were incubated with 1 mL Congo Red solution (0.035 g/L Congo Red, 5 mM potassium phosphate, 150 mM NaCl, pH 7.4) for 30 min, or with 1 mL ThT solution (0.016 g/L ThT, 10 mM phosphate, 150 mM NaCl, pH 7.4). The absorbance spectrum of the peptide/Congo Red mixture was recorded between 400 and 700 nm, and the spectrum of the Congo Red solution mixed with 10 μ L DMSO subtracted. The fluorescence emission spectrum of the peptide/ThT mixture was recorded between 460 nm and 540 nm with a bandwidth of 10 nm and an excitation wavelength at 440 nm.

2.8. Immunofluorescence staining

293T cells were transiently transfected with pcDNA3.1-OPTS-HA or pXJ40-S, with or without pre-infection with recombinant vaccinia virus-T7 (VTF7.3) (MOI = 1), respectively, using Lipofectamine 2000 (Life Technologies, Singapore). Twenty-four h post-transfection, cells were fixed with 4% paraformaldehyde and permeabilized with 0.5% Triton X-100. Cells were co-stained with 2 μ M C6 and anti-HA (Y-11) or anti-S antibody (Lu et al., 2008b), followed by Dylight 488-conjugated NeutrAvidin™ (Thermo Fisher Scientific) and Alexa 594-conjugated anti-rabbit antibody (Molecular Probes) for anti-HA primary staining or Alexa 488-conjugated anti-mouse antibody for anti-S primary staining.

Slides were mounted in Prolong Gold Anti-Fade medium with DAPI (Invitrogen), and analyzed with an Axiovert 200M inverted fluorescence compound microscope (Carl Zeiss, Germany).

3. Results & discussion

3.1. Peptide array mapping of S1188HA-binding sequences

To map putative self-binding sequences within the S protein, peptide array libraries of overlapping 15- to 20-residue peptides with offsets of two to four residues were derived from SARS-CoV S protein (Frank, 2002; Frank and Overwin, 1996), synthesized on PEG-derivatized cellulose membranes, and then probed by S1188HA, a recombinant HA-tagged S protein ectodomain (aa 1-1188) that is structurally more stable than the full length S protein (Lu et al., 2008a). S1188HA in this study was expressed in the Sf9 insect cell system, based on the observations that the Sf9 insect cell offered higher expression level of S1188HA without affecting the protein immunogenicity, receptor-binding properties or its ability to construct virus-like particles, as compared to the mammalian system (Jeffers et al., 2004; Mortola and Roy, 2004). Peptide-retained S1188HA was then detected as dark spots on the membranes by an anti-HA chemiluminescence immunodetection (Supplementary S1 Fig.). False-positive sequences were identified by immunoblotting the peptide-anchored membranes with an HRP-conjugated secondary antibody alone or in combination with a primary anti-HA antibody, without probing the membranes with S1188HA (S2 Fig.). Neighboring overlapping peptides that did not bind to S1188HA served as negative controls, further ensuring the specificities of the peptide-S1188HA interactions.

Based on primary screening data using libraries of different peptide lengths, the 20-residue peptide library with an offset of 4 aa provided the most comprehensive hit peptide profile, and was chosen for further study. In brief, probing 310 peptides in the 20-residue library with S1188HA identified thirty-four S1188HA-binding peptides, sequences of which were located to the N-terminal region of S1, RBD, the region between S1 and S2, IFP, HR1, and the loop region connecting HRs (Fig. 1a and Table 1). Additionally, these identified peptides appeared in clusters. Five clusters shared a common feature of containing three to four overlapping peptides, each yielding a consensus putative self-binding octapeptide motif (Fig. 1b and Table 1). These were the motif GINITNFR (aa 225-232) in Cluster I peptides C6–C9 derived from the region upstream to the RBD; the motif VLTSPSKR (aa 537-544) in Cluster II peptides F12–F15 derived from the region immediately following RBD; the motif LNRALSGI (aa 745-752) in Cluster III peptides H16, 18 and 19 derived from the region upstream of FP; the motif AMQMAYRF (aa 881-888) in Cluster IV peptides J2, 3 and 5 derived from IFP; and finally, the motif RLITGRQLQ (aa 977-984) in Cluster V peptides K2-K5 derived from the HR1 (Table 1). Besides the five continuous clusters of self-binding peptides, the sixth cluster R contained a cluster of eight discontinuous RBD-derived sequences that bound to S1188HA with relatively high affinities.

It was also noted that no HR2- and only four HR1-derived sequences, K2, K3, K4 and K5, were identified as putative self-binding sequences from the 20-residue peptide array library. The HR regions of Class 1 viral fusion glycoproteins, including SARS-CoV S protein, are known to oligomerize into helix trimers through Leu/Ile zippers (Hakansson-McReynolds et al., 2006; Xu et al., 2004). Accordingly, peptide GG38, encompassing the entire S protein HR2 sequence (aa 1149-1186), both oligomerized into α helix trimers and heteromerized with the HR1 peptide into the 6-HB (Bosch et al., 2004; Celigoy et al., 2011) (S3 Fig.). The discrepancy between the known oligomerization potential of the HR sequences and their underrepresentation among self-binding peptides identified in this study may be due to that our peptide array of 20-aa length, which while well suited to identify short-sequence-mediated self-interactions (e.g. steric β -zipper), is inadequate to sustain helix-mediated interactions. This was confirmed by the

Table 1

Putative self-binding peptides identified by scanning the S protein-derived 20-residue peptide array library.

Cluster	Peptide	Sequence	Position (Domain)
I	A6	TFDDVQAPNYTQHTSSMRGV	21 – 40
	A8	NYTQHTSSMRGVYYPDEIFR	29 – 48
	C6	FNTLKPIFKLPLGINITNFR ^a	213 – 232
	C7	KPIFKLPLGINITNFRAILT	217 – 236
	C8	KLPLGINITNFRAILTAFSP	221 – 240
	C9	GINITNFRAILTAFSPAQDI	225 – 244
R	D1	SVKSFEDKGIYQTSNFRV	289 – 308
	D4	QTSNFRVPSGDVVRFPNIT	301 – 320 (RBD)
	D14	ERKKISNCVADYSVLYNSTF	341 – 360 (RBD)
	D23	LCFSNVYADSFVVKGDVDRQ	377 – 396 (RBD)
	D24	NVYADSFVVKGDVDRQIAPG	381 – 400 (RBD)
	E7	NYKLPDDFMGCVLAWNTRNI	409 – 428 (RBD)
	E11	TRNIDATSTGNINYKYRYLR	425 – 444 (RBD)
	E13	TGNINYKYRYLRHGKLRPFE	433 – 452 (RBD)
	E24	PLNDYGFYTTTGGYQPYRV	477 – 496 (RBD)
	II	F12	VNFNFGTLTGTGLTPSSKR
F13		FNGTLTGTGLTPSSKRFQPF	529 – 548
F14		TGTGLTPSSKRFQPFQFG	533 – 552
F15		VLTSPSKRFQPFQFGRDVS	537 – 556
H13		NMYICGDSTECANLLQYGS	721 – 740
III	H16	NLLLYQGSFCTQLNRALSGI	733 – 752
	H18	FCTQLNRALSGIAEQDRNT	741 – 760
	H19	LNRALSGIAEQDRNTREVF	745 – 764
IV	J2	TFGAGAAALQIPFAMQMAYRF	869 – 888 (IFP)
	J3	GAALQIPFAMQMAYRFNGIG	873 – 892 (IFP)
	J5	AMQMAYRFNGIGVTONVLYE	881 – 900 (IFP)
V	K2	RLDKVEAEVQIDRLITGRQLQ	965 – 984 (HR1)
	K3	VEAEVQIDRLITGRQLQSLQT	969 – 988 (HR1)
	K4	VQIDRLITGRQLQSLQTYVTQ	973 – 992 (HR1)
	K5	RLITGRQLQSLQTYVTQQLIR	977 – 996 (HR1)
	L5	REGVVFVNGTSWFIQTRNFF	1073 – 1092 (Loop)
L6	FVFNGTSWFIQTRNFFSPQI	1077 – 1096 (Loop)	
L8	FITQRNFFSPQIITDNTFV	1085 – 1104 (Loop)	
L12	NTFVSGNCDVVIGIINNTVY	1101 – 1120 (Loop)	

^aConsensus putative self-binding sequences were underlined.

diminished ability of HR2-derived peptides to pull down S1188HA, when subjected to serial C-terminal truncation (S4 Fig.) (Jiang and Lin, 1995).

3.2. S protein-derived peptides pulled down S1188HA putatively through homo-oligomerization

To confirm and investigate the peptide-S protein interaction, 8 representative peptides, C6, D4A, D24, E11, H18A, J1A, K2A and K4A, were synthesized and applied in pull down experiments. These eight peptides were chosen based on their relatively high affinity to S1188HA in peptide array screening and their inclusion of the consensus self-binding sequences (Table 2). Peptide D4A (302 to 321 aa) contained the sequence shifted downstream from the scanning-identified D4 sequence, to facilitate peptide synthesis and purification. The scanning-identified H18 sequence contained an N-terminal cysteine residue. To investigate if the H18-S protein interaction was mediated through

Table 2

Biotinylated S protein-derived peptides synthesized for the pull down experiments.

Peptide	Sequence	Position (domain)
C6	FNTLKPIFKLPLGINITNFR	213-232
D4A	TSNFRVPSGDVVRFPNITN	302-321 (RBD)
D24	NVYADSFVVKGDVDRQIAPG	381-400 (RBD)
E11	TRNIDATSTGNINYKYRYLR	425-444 (RBD)
H18A	TQLNRALSGIAEQDRNTR	743-762
J1A	AGWTFGAGAAALQIPFAMQMAYRF	866-888 (IFP)
K2A	RLDKVEAEVQIDRLITGRQLQSLQT	965-988 (HR1)
K4A	VQIDRLITGRQLQSLQTYVTQQLIR	973-996 (HR1)
GG38	GDISGINASVSVNIQKEIDRLNEVAKNLNLSLIDLQELG	1149-1186 (HR2)

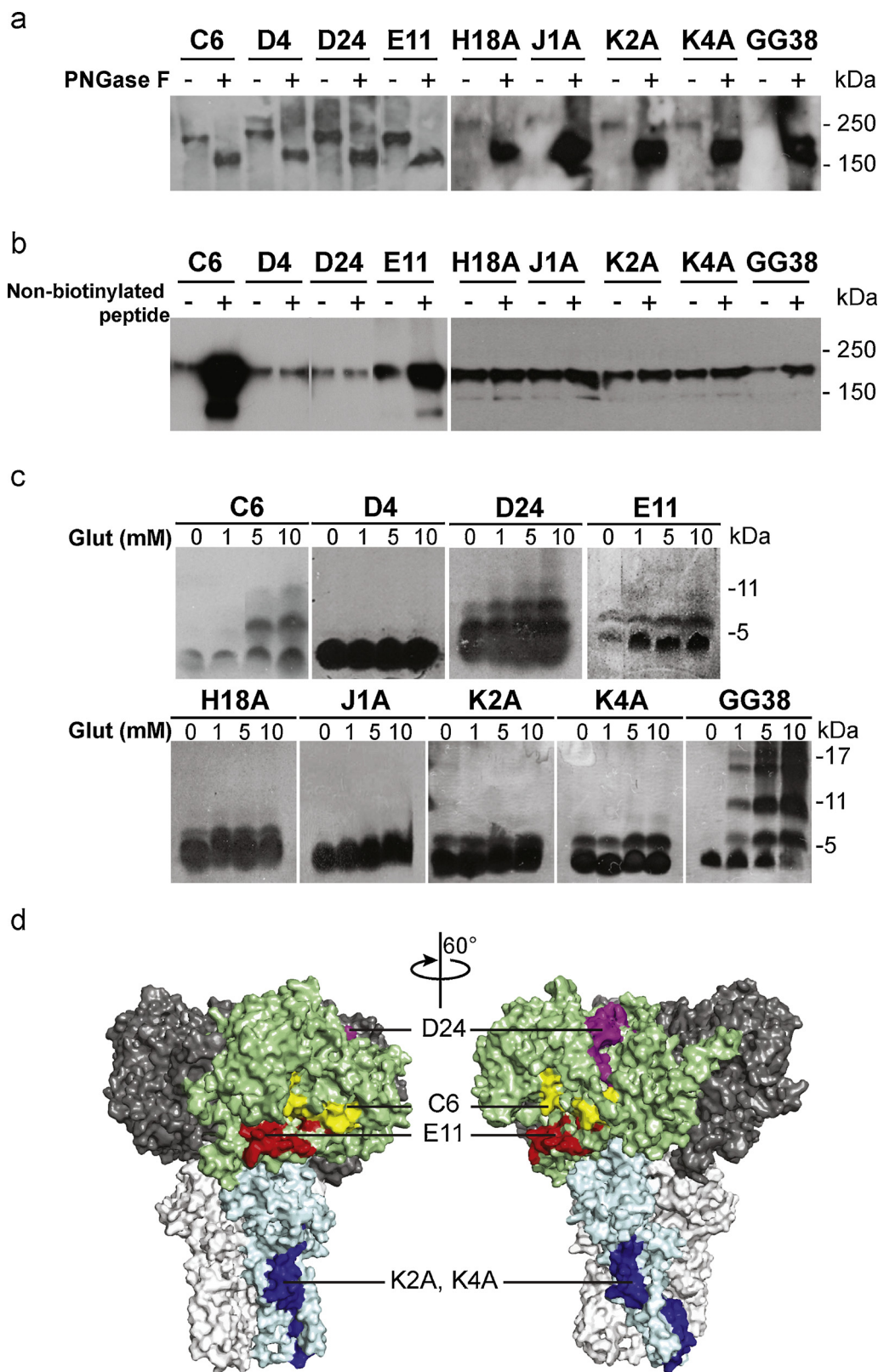


Fig. 2. Identification of peptides containing oligomerization motifs. **a.** Biotinylated S protein-derived peptides pulled down the deglycosylated S1188HA. **b.** Biotinylated S protein-derived peptides C6, E11, K2A, K4A and GG38 pulled down enhanced amount of S1188HA, when Sf9 cell lysate was pre-incubated with the respective non-biotinylated peptides. **c.** Peptide C6, D24, E11, K2A, K4A and GG38 oligomerized in crosslinker glutaraldehyde. **d.** The identified oligomerizing sequences C6, D24, E11, K2A and K4A were mapped to the surface-exposed regions on the model structure of the S protein trimer (PDB: 1T7G). One S1 subunit was in pale green and one S2 subunit in pale blue, while the rest of two S1 and S2 subunits in dark and light grey, respectively. (For interpretation of the references to colour in this figure legend, the reader is referred to the web version of this article).

disulfide bond formation, peptide H18A (743 to 762 aa) with sequence shifted downstream from the H18 by two residues was generated. Peptide J1A (866 to 888 aa) contained sequences of the overlapping J1 and J2 peptides that were identified from the 15-residue and 20-residue peptide array library, respectively. Finally, peptide K2A contains sequences of the overlapping K2 and K3 sequences, while K4A contains

sequences of the overlapping K4 and K5 sequences. Each of these eight peptides was entirely or largely composed of sequences identified from peptide array scanning, where the specificities of their interactions with S1188HA were ensured by including continuous overlapping peptides. Therefore, no scrambled peptide was included in the subsequent pull down experiments. Finally, peptide GG38 (aa 1149-1186), which was

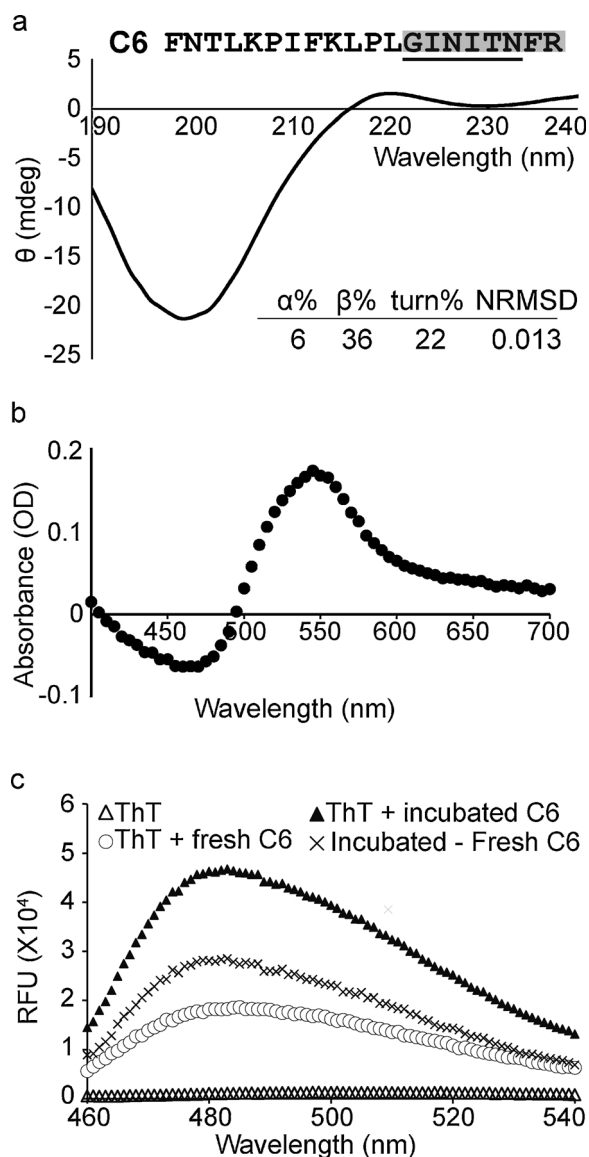


Fig. 3. Peptide C6 exhibited characteristics of amyloid-like fibrils. **a.** Peptide C6 contained a predicted amyloid-like fibril-forming segment and exhibited β -strand content in an aqueous environment. The Cluster I consensus sequence is in bold and the predicted amyloid-like fibril-forming segment underlined. The CD spectrum of C6 (1 mM) in H₂O was shown with its estimated secondary structure contents. NRMSD, normalized root mean square deviation. **b.** The aged C6 exhibited maximal absorbance at 540 nm when mixed with Congo Red. **c.** The aged C6 had an increased fluorescence emission at 482 nm, when mixed with ThT.

derived from the oligomerizing S protein HR2 sequence, served as the positive control for the S protein-derived self-binding peptide in the following pull down experiments.

Consistent with the scanning results, all eight peptides plus the control GG38 peptides pulled down the S1188HA protein from the Sf9 cell lysates (Fig. 2a). The S protein is heavily glycosylated with 23 potential N-linked glycosylation sites (Ying et al., 2004). By using S1188HA-containing lysate pretreated with PNGase F that removes the N-linked glycans, we could show that all eight peptides pulled down the PNGase-F-treated S1188HA, similarly to the control peptide GG38, suggesting that these peptides bound to the S protein through amino acid sequence- but not glycan-mediated interactions (Fig. 2a). We further observed that the peptides C6, E11, K2A and K4A, and the positive control peptide GG38 pulled down greater amount of S1188HA, when

the cell lysates were pre-treated with their respective non-biotinylated analogues (Fig. 2b). A possible explanation for this phenomenon is that the peptides C6, E11, K2A and K4A contained oligomerization sequences, as does the positive control HR2 peptide GG38, which contains a trimerizing sequence (Celigoy et al., 2011; Hakansson-McReynolds et al., 2006). The potential oligomerization sequences within C6, E11, K2A and K4A could enable the non-biotinylated peptides to bind to S1188HA during pre-treatment, and further serve as oligomerization sites for their biotinylated analogues during pull down experiments. These oligomerization sequences within the non-biotinylated peptides would be more exposed and accessible than the corresponding region within S1188HA, which could serve as a 'bridge' between the biotinylated peptides and S1188HA and thereby lead to an enhanced retention of S1188HA.

To strengthen our evidence for the oligomerization potential of the self-binding peptides C6, E11, K2A and K4A, chemical crosslinking experiments were performed. With increasing concentrations of the chemical crosslinker glutaraldehyde, peptides C6, D24 and E11 subsequently formed dimer, trimer, and higher-order oligomers, in the same way as the HR2 control peptide GG38 (Fig. 2c). We also observed that the HR1-derived peptides K2A and K4A formed dimers under chemical crosslinking experiments, consistent with observation in previous studies by others [46] and by our group (S5 Fig.) that HR1 sequences can oligomerize (Supekar et al., 2004). However, we did not observe any higher-order oligomers even at relatively high concentrations of the chemical crosslinker (Fig. 2c), possibly owing to their incomplete inclusion of the HR1 sequence.

Our data suggest that the peptides C6, D24, E11, K2A and K4A self-adhered to S1188HA through a sequence-based, not glycan-dependent, and likely homophilic-interaction-mediated mechanism. All of these oligomerizing peptides, C6, D24, E11, K2A and K4A, were mapped onto the surface exposed regions within the S protein model structure (PDB: 1T7G) (Fig. 2d) (Spiga et al., 2003). Furthermore, most of them have been shown to contain potential antigenic epitopes, which further confirms that these sequences are located in the accessible regions on the S protein (S1 Table) (Duan et al., 2005; Greenough et al., 2005; He et al., 2006, 2005; He et al., 2004). Their homophilic-interaction potential and the accessibility of their corresponding regions on the S protein indicated that these peptides could bind to S protein during viral infection and potentially be used as viral detection reagents, particularly if the peptide-S protein interactions are maintained through sequence-specific interactions such as the β -zipper motifs within amyloid-like fibrils. Indeed, amyloid-derived steric β -zipper peptides have been shown to specifically bind to the cognate amyloid protein through oligomerization with the corresponding sequence within the protein (Hard and Lendel, 2012).

3.3. Peptide C6 formed amyloid-like fibrils potentially through a steric β -zipper motif

We next identified the β -zipper-like self-binding peptides within the S protein by sequentially predicting β -zipper segments and then comparing the prediction results with the peptide array scanning results. The S protein-derived peptides with high potential to form steric β -zippers, or the self-complementary motif between facing β -sheets that enables amyloid-like fibrillation, were predicted by the 3D profile method developed by the Eisenberg group (Bowie et al., 1991; Goldschmidt et al., 2010; Thompson et al., 2006); and followed by assessing β -sheet-favorable residue pairings within the peptide self-dimers using pair correlation data from the work of Wouters and Curmi (Wouters and Curmi, 1995). Among the peptides that oligomerized under chemical crosslinking, both C6 and E11 could form multiple residue pairings that were positively correlated with antiparallel β -sheet formation (S7 Fig.), and were further predicted to contain steric β -zipper-like fibril-forming segments.

Particularly, the Cluster I consensus sequence, GINITNFR within C6

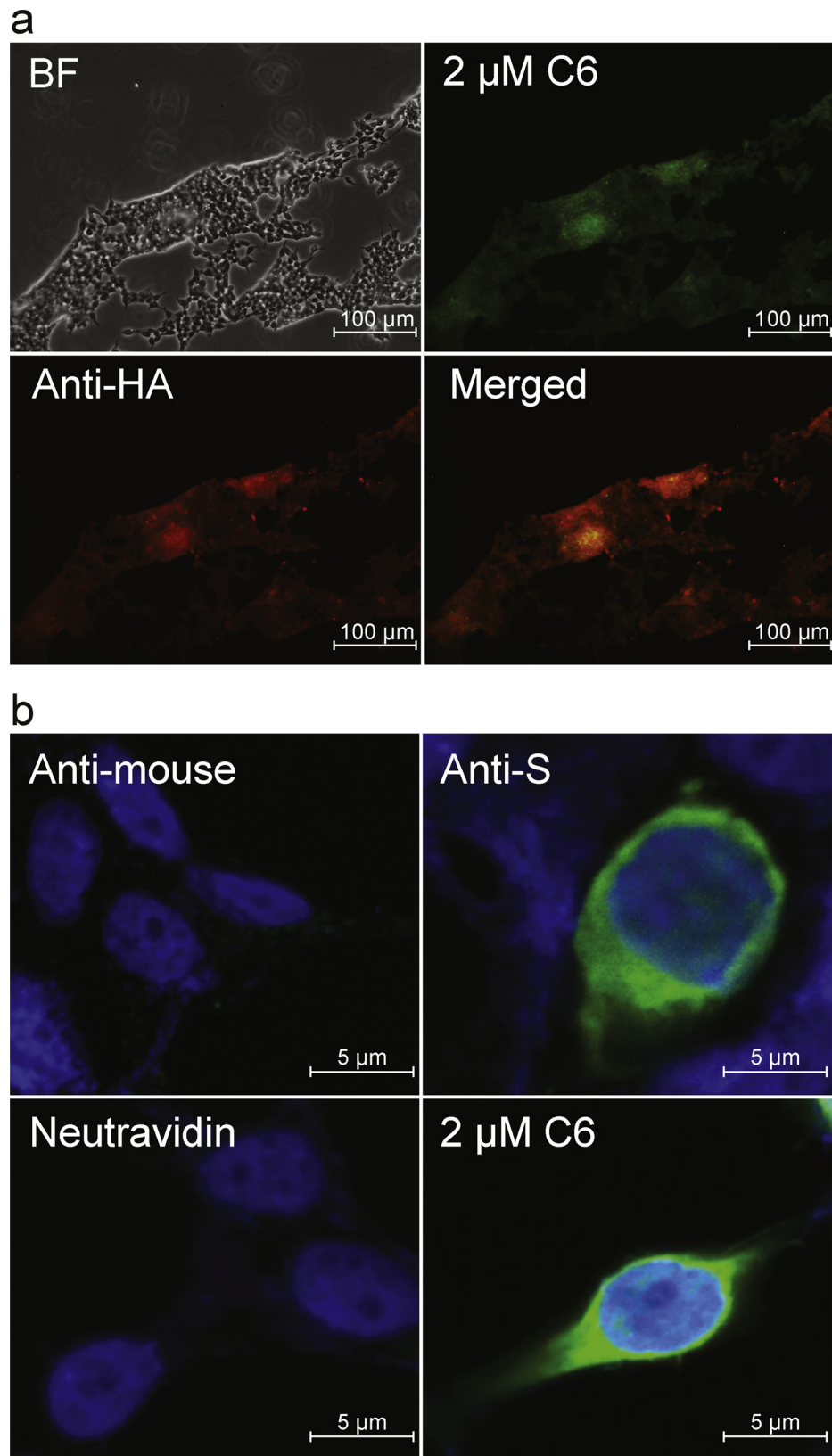


Fig. 4. C6 detected the expression of full-length S protein in 293T cells and the effect of peptide homodimerization on C6-S1188HA interaction. a. Peptide C6 and anti-HA antibodies co-stained 293T cells that were transiently expressing HA-tagged full-length S protein. b. Peptide C6 had the same staining pattern of 293T cells that were transiently expressing full-length S protein, as an anti-S monoclonal antibody did. Control cells were stained with the fluorescein-conjugated secondary antibodies only.

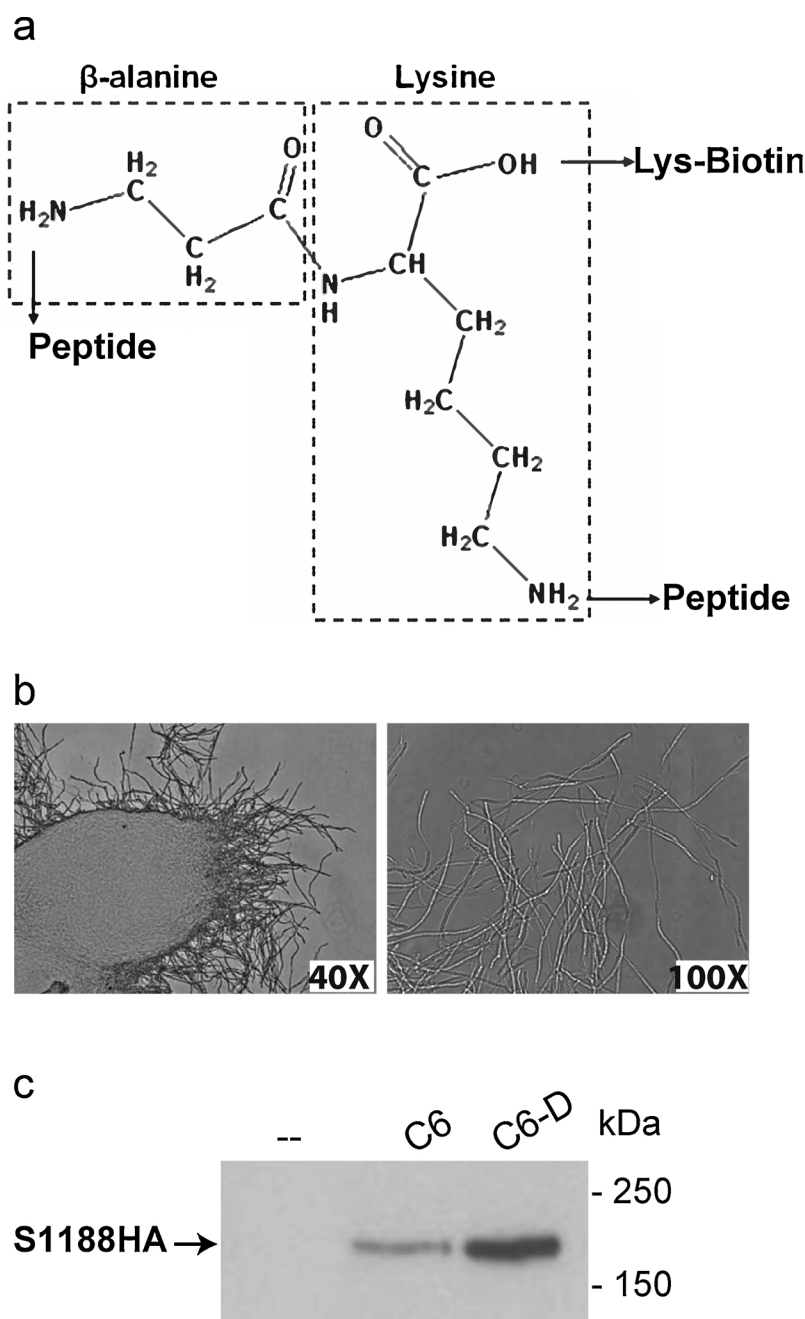


Fig. 5. Peptide C6-S1188HA interaction avidity could be enhanced through homodimerization of peptide C6. **a.** Lys-based linker molecule for the synthesis of C6-D. **b.** C6-D aggregated and formed fibril-like network, as observed under light microscopy at 40 \times (left), and 100 \times (right) magnifications. **c.** C6-D had enhanced pull-down efficiency of S1188HA than C6.

showed similar charge distribution and side chain sizes as the steric β -zipper-like amyloid-forming sequence GNNQQNY (Nelson et al., 2005), and its partial sequence GINITNF was predicted to be fibril-forming (Fig. 3a). Subsequently, the structural profile and fibrillation behavior of C6 was investigated, using CD spectroscopy and Congo red and thioflavin T (ThT) spectroscopic assays, respectively. Peptide C6 was dissolved at 10 mg/ml, a relatively high concentration that could accelerate nucleation stage and allow the observation of fibrillation within the experiment time-span of three days (Teng and Eisenberg, 2009). It has been previously shown that amyloid-like fibrils could bind to Congo Red, resulting in characteristic apple-green birefringence under polarized light and enhanced absorbance at 540 nm (Nilsson, 2004). It is shown here that peptide C6, upon 3-day incubation,

exhibited an increase of absorbance at 540 nm when mixed with Congo Red, suggesting its Congo red-binding and fibrillation formation behavior (Fig. 3b). The incubated peptide C6 also resulted in an approximately 2.5 times increase of the fluorescence emission at 482 nm when mixed with ThT, another characteristic behavior of amyloid fibrils (Biancalana and Koide, 2010; Nilsson, 2004), further confirming its ability to form amyloid-like fibrils (Fig. 3c). Furthermore, CD spectroscopy study revealed that C6 adopts a β -strand conformation in aqueous environment, supporting its ability to form β -strand-containing structures such as the β -zipper (Fig. 3a). Meanwhile, the other potentially amyloidogenic peptide E11 did not demonstrate these amyloid-like characteristics (S6 Fig.).

3.4. Peptide C6 could detect S protein expression and homodimerization enhanced its affinity to S1188HA

Taking advantage of its self-interacting amyloidogenic behavior, C6 was further applied to detect S protein expression by fluorescence staining in 293 T cells, a human embryonic kidney cell line permissive to SARS-CoV infection (Gillim-Ross et al., 2004). The 293 T cells transiently expressing an HA-tagged full-length S protein, were stained with either anti-HA (Y-11) primary antibody followed by Alexa Fluor 594-conjugated secondary antibody (Fig. 4a, panel 'anti-HA'), or with 2 μ M of the biotinylated peptide C6 followed by Dylight 488-conjugated Neutravidin™ (Fig. 4a, panel '2 μ M C6'). The staining pattern of anti-HA antibody targeting the S protein, and that of fluorescence-conjugated Neutravidin™ targeting the C6 peptide, were found to co-localize (Fig. 4a). The cells expressing high levels of the S protein were also bound extensively by peptide C6 (Fig. 4a). We further applied C6 and anti-S antibody separately to detect the expression of an un-tagged full-length S protein (S1255). 293 T cells transiently expressing S1255 were subjected to fluorescence staining using either a conventional mouse anti-S monoclonal antibody as the primary antibody and then an Alexa Fluor 488-conjugated donkey anti-mouse secondary antibody, or using a 2 μ M peptide C6 followed by Dylight 488-conjugated Neutravidin™. Control cells were probed with fluorescein-conjugated secondary antibody or Neutravidin™ alone. C6 detected S1255 expression in 293 T cells, with the staining pattern and intensity similar to that obtained with the anti-S monoclonal antibody (Fig. 4b). As our first step to enhance the binding avidity of peptide C6 to S1188HA, C6 was homodimerized on a biotinylated Lys-based linker molecule, a strategy that has been applied successfully in enhancing the peptide immunogenicity and anti-viral potency (Fig. 5a) (Tam, 1988; Tam et al., 2002). The dimeric C6 peptide, C6-D, formed visible fibril-like aggregates upon four to five days of incubation at 4 °C (Fig. 5b). However, such aggregates were not observed in C6 monomer when incubated for the same duration at 4 °C. Furthermore, in the pull down experiment, peptide C6-D retained approximately 2.5 times higher amount of S1188HA than C6 (Fig. 5c). Collectively, the data indicate that the dimeric C6-D had a higher propensity for oligomerization and a stronger affinity towards the S protein, as compared to the monomeric C6, which warrants further investigation of C6-D as a detection reagent for S protein expression.

4. Conclusions

The data presented in this paper demonstrate that β -zipper-like self-binding peptides, which bind to the protein-of-origin by forming sequence-specific steric β -zippers, could be identified by employing peptide scanning and zipper sequence prediction using programs such as the 3D profile method. Self-binding peptides, such as C6 from SARS-CoV S protein, might mimic certain functions of an antibody for protein detection. With an enhanced peptide-protein interaction avidity and specificity, this approach may be further developed as an animal-free way to rapidly generate and produce peptide-based viral diagnostic and research tools.

Acknowledgements

This research was in part supported by the Singapore Ministry of Education AcRF Tier 3 funding (MOE2016-T3-1-003) and the Singapore Ministry of Education AcRF Tier 2 funding (ACR47/14).

Appendix A. Supplementary data

Supplementary material related to this article can be found, in the online version, at doi: <https://doi.org/10.1016/j.biocel.2018.05.012>.

References

- Azrieli, R., Gazit, E., 2001. Analysis of the minimal amyloid-forming fragment of the Iset amyloid polypeptide: an experimental support for the key role of the phenylalanine residue in amyloid formation. *J. Biol. Chem.* 276 (36), 34156–34161.
- Azzarito, V., Long, K., Murphy, N.S., Wilson, A.J., 2013. Inhibition of alpha-helix-mediated protein-protein interactions using designed molecules. *Nat. Chem.* 5 (3), 161–173.
- Balbach, J.J., Ishii, Y., Antzutkin, O.N., Leapman, R.D., Rizzo, N.W., Dyda, F., Reed, J., Tycko, R., 2000. Amyloid fibril formation by A β 16–22, a seven-residue fragment of the Alzheimer's β -amyloid peptide, and structural characterization by solid state NMR†. *Biochemistry* 39 (45), 13748–13759.
- Balbirnie, M., Grothe, R., Eisenberg, D.S., 2001. An amyloid-forming peptide from the yeast prion Sup35 reveals a dehydrated beta-sheet structure for amyloid. *Proc. Natl. Acad. Sci. U. S. A.* 98 (5), 2375–2380.
- Beisswenger, M., Cabrele, C., 2014. Self-recognition behavior of a helix-loop-helix domain by a fragment scan. *Biochim. Biophys. Acta* 1844 (9), 1675–1683.
- Biancalana, M., Koide, S., 2010. Molecular mechanism of Thioflavin-T binding to amyloid fibrils. *Biochim. Biophys. Acta* 1804 (7), 1405–1412.
- Borrego, P., Calado, R., Marcelino, J.M., Pereira, P., Quintas, A., Barroso, H., Taveira, N., 2013. An ancestral HIV-2/simian immunodeficiency virus peptide with potent HIV-1 and HIV-2 fusion inhibitor activity. *Aids* 27 (7), 1081–1090.
- Bosch, B.J., Martina, B.E., Van Der Zee, R., Lepault, J., Haijema, B.J., Versluis, C., Heck, A.J., De Groot, R., Osterhaus, A.D., Rottier, P.J.M., 2004. Severe acute respiratory syndrome coronavirus (SARS-CoV) infection inhibition using spike protein heptad repeat-derived peptides. *Proc. Natl. Acad. Sci. U. S. A.* 101 (22), 8455–8460.
- Bosch, B.J., van der Zee, R., de Haan, C.A.M., Rottier, P.J.M., 2003. The coronavirus spike protein is a Class I virus fusion protein: structural and functional characterization of the fusion core complex. *J. Virol.* 77 (16), 8801–8811.
- Bowie, J.U., Luthy, R., Eisenberg, D., 1991. A method to identify protein sequences that fold into a known three-dimensional structure. *Science* 253 (5016), 164–170.
- Celigoy, J., Ramirez, B., Caffrey, M., 2011. SARS-CoV heptad repeat 2 is a trimer of parallel helices. *Protein Sci. : Publ. Protein Soc.* 20 (12), 2125–2129.
- Chen, Z., Zhang, L., Qin, C., Ba, L., Yi, C.E., Zhang, F., Wei, Q., He, T., Yu, W., Yu, J., Gao, H., Tu, X., Gettie, A., Farzan, M., Yuen, K.-y., Ho, D.D., 2005. Recombinant modified vaccinia virus Ankara expressing the spike glycoprotein of severe acute respiratory syndrome coronavirus induces protective neutralizing antibodies primarily targeting the receptor binding region. *J. Virol.* 79 (5), 2678–2688.
- Cochran, A.G., Skelton, N.J., Starovasnik, M.A., 2001. Tryptophan zippers: stable, monomeric beta-hairpins. *Proc. Natl. Acad. Sci. U. S. A.* 98 (10), 5578–5583.
- Duan, J., Yan, X., Guo, X., Cao, W., Han, W., Qi, C., Feng, J., Yang, D., Gao, G., Jin, G., 2005. A human SARS-CoV neutralizing antibody against epitope on S2 protein. *Biochem. Biophys. Res. Commun.* 333 (1), 186–193.
- Frank, R., 2002. The SPOT-synthesis technique. Synthetic peptide arrays on membrane supports—principles and applications. *J. Immunol. Methods* 267 (1), 13–26.
- Frank, R., Overwin, H., 1996. SPOT synthesis. Epitope analysis with arrays of synthetic peptides prepared on cellulose membranes. *Methods Mol. Biol.* 66, 149–169.
- Giannecchini, S., Alcaro, M.C., Isola, P., Sichi, O., Pistello, M., Papini, A.M., Rovero, P., Bendinelli, M., 2005. Feline immunodeficiency virus plasma load reduction by a retroinverso octapeptide reproducing the Trp-rich motif of the transmembrane glycoprotein. *Antivir. Ther.* 10 (5), 671–680.
- Gillim-Ross, L., Taylor, J., Scholl, D.R., Ridenour, J., Masters, P.S., Wentworth, D.E., 2004. Discovery of novel human and animal cells infected by the severe acute respiratory syndrome coronavirus by replication-specific multiplex reverse transcription-PCR. *J. Clin. Microbiol.* 42 (7), 3196–3206.
- Goldschmidt, L., Teng, P.K., Riek, R., Eisenberg, D., 2010. Identifying the amyloids, proteins capable of forming amyloid-like fibrils. *Proc. Natl. Acad. Sci. U. S. A.* 107 (8), 3487–3492.
- Greenough, T.C., Babcock, G.J., Roberts, A., Hernandez, H.J., Thomas Jr., W.D., Coccia, J.A., Graziano, R.F., Srinivasan, M., Lowy, I., Finberg, R.W., Subbarao, K., Vogel, L., Somasundaran, M., Luzuriaga, K., Sullivan, J.L., Ambrosino, D.M., 2005. Development and characterization of a severe acute respiratory syndrome-associated coronavirus-neutralizing human monoclonal antibody that provides effective immunoprophylaxis in mice. *J. Infect. Dis.* 191 (4), 507–514.
- Guillen, J., Perez-Berna, A.J., Moreno, M.R., Villalain, J., 2008. A second SARS-CoV S2 glycoprotein internal membrane-active peptide. Biophysical characterization and membrane interaction. *Biochemistry* 47 (31), 8214–8224.
- Hakansson-McReynolds, S., Jiang, S., Rong, L., Caffrey, M., 2006. Solution structure of the severe acute respiratory syndrome-coronavirus heptad repeat 2 domain in the prefusion state. *J. Biol. Chem.* 281 (17), 11965–11971.
- Hakoshima, T., 2001. Leucine Zippers. eLS. John Wiley Sons, Ltd.
- Hard, T., Lendel, C., 2012. Inhibition of amyloid formation. *J. Mol. Biol.* 421 (4–5), 441–465.
- He, Y., Li, J., Heck, S., Lustigman, S., Jiang, S., 2006. Antigenic and immunogenic characterization of recombinant baculovirus-expressed severe acute respiratory syndrome coronavirus spike protein: implication for vaccine design. *J. Virol.* 80 (12), 5757–5767.
- He, Y., Lu, H., Siddiqui, P., Zhou, Y., Jiang, S., 2005. Receptor-binding domain of severe acute respiratory syndrome coronavirus spike protein contains multiple conformation-dependent epitopes that induce highly potent neutralizing antibodies. *J. Immunol.* 174 (8), 4908–4915.
- He, Y., Zhou, Y., Wu, H., Luo, B., Chen, J., Li, W., Jiang, S., 2004. Identification of immunodominant sites on the spike protein of severe acute respiratory syndrome (SARS) coronavirus: implication for developing SARS diagnostics and vaccines. *J. Immunol.* 173 (6), 4050–4057.

- Jeffers, S.A., Tusell, S.M., Gillim-Ross, L., Hemmila, E.M., Achenbach, J.E., Babcock, G.J., Thomas Jr., W.D., Thackray, L.B., Young, M.D., Mason, R.J., Ambrosino, D.M., Wentworth, D.E., Demartini, J.C., Holmes, K.V., 2004. CD209L (L-SIGN) is a receptor for severe acute respiratory syndrome coronavirus. *Proc. Natl. Acad. Sci. U. S. A.* 101 (44), 15748–15753.
- Jiang, S., Lin, K., 1995. Effect of amino acid replacements, additions and deletions on the antiviral activity of a peptide derived from the HIV-1 GP41 sequence. *Pept. Res.* 8 (6), 345–348.
- Kaukinen, P., Vaheiri, A., Plyusnin, A., 2003. Mapping of the regions involved in homotypic interactions of Tula hantavirus N protein. *J. Virol.* 77 (20), 10910–10916.
- Liao, Y., Zhang, S.M., Neo, T.L., Tam, J.P., 2015. Tryptophan-dependent membrane interaction and heteromerization with the internal fusion peptide by the membrane proximal external region of SARS-CoV spike protein. *Biochemistry* 54 (9), 1819–1830.
- Liu, S., Lu, H., Niu, J., Xu, Y., Wu, S., Jiang, S., 2005. Different from the HIV fusion inhibitor C34, the anti-HIV drug Fuzeon (T-20) inhibits HIV-1 entry by targeting multiple sites in gp41 and gp120. *J. Biol. Chem.* 280 (12), 11259–11273.
- Liu, S., Xiao, G., Chen, Y., He, Y., Niu, J., Escalante, C.R., Xiong, H., Farmar, J., Debnath, A.K., Tien, P., Jiang, S., 2004. Interaction between heptad repeat 1 and 2 regions in spike protein of SARS-associated coronavirus: implications for virus fusogenic mechanism and identification of fusion inhibitors. *Lancet* 363 (9413), 938–947.
- Lu, Y., Liu, D.X., Tam, J.P., 2008a. Lipid rafts are involved in SARS-CoV entry into Vero E6 cells. *Biochem. Biophys. Res. Commun.* 369 (2), 344–349.
- Lu, Y., Neo, T.L., Liu, D.X., Tam, J.P., 2008b. Importance of SARS-CoV spike protein Trp-rich region in viral infectivity. *Biochem. Biophys. Res. Commun.* 371 (3), 356–360.
- Medinas, R.J., Lambert, D.M., Tompkins, W.A., 2002. C-Terminal gp40 peptide analogs inhibit feline immunodeficiency virus: cell fusion and virus spread. *J. Virol.* 76 (18), 9079–9086.
- Mortola, E., Roy, P., 2004. Efficient assembly and release of SARS coronavirus-like particles by a heterologous expression system. *FEBS Lett.* 576 (1–2), 174–178.
- Nelson, R., Sawaya, M.R., Balbirnie, M., Madsen, A.O., Riekel, C., Grothe, R., Eisenberg, D., 2005. Structure of the cross-beta spine of amyloid-like fibrils. *Nature* 435 (7043), 773–778.
- Nilsson, M.R., 2004. Techniques to study amyloid fibril formation in vitro. *Methods* 34 (1), 151–160.
- Parry, D.A., 2005. Structural and functional implications of sequence repeats in fibrous proteins. *Adv. Protein Chem.* 70, 11–35.
- Perutz, M., 1994. Polar zippers: their role in human disease. *Protein Sci. : Publ. Protein Soc.* 3 (10), 1629–1637.
- Reches, M., Porat, Y., Gazit, E., 2002. Amyloid fibril formation by pentapeptide and tetrapeptide fragments of human calcitonin. *J. Biol. Chem.* 277 (38), 35475–35480.
- Rigter, A., Langeveld, J.P., Timmers-Parohi, D., Jacobs, J.G., Moonen, P.L., Bossers, A., 2007. Mapping of possible prion protein self-interaction domains using peptide arrays. *BMC Biochem.* 8, 6.
- Sawaya, M.R., Sambashivan, S., Nelson, R., Ivanova, M.I., Sievers, S.A., Apostol, M.I., Thompson, M.J., Balbirnie, M., Wiltzius, J.J., McFarlane, H.T., Madsen, A.O., Riekel, C., Eisenberg, D., 2007. Atomic structures of amyloid cross-beta spines reveal varied steric zippers. *Nature* 447 (7143), 453–457.
- Spiga, O., Bernini, A., Ciutti, A., Chiellini, S., Menciasci, N., Finetti, F., Causarono, V., Anselmi, F., Prischi, F., Niccolai, N., 2003. Molecular modelling of S1 and S2 subunits of SARS coronavirus spike glycoprotein. *Biochem. Biophys. Res. Commun.* 310 (1), 78–83.
- Supekar, V.M., Bruckmann, C., Ingallinella, P., Bianchi, E., Pessi, A., Carfi, A., 2004. Structure of a proteolytically resistant core from the severe acute respiratory syndrome coronavirus S2 fusion protein. *Proc. Natl. Acad. Sci.* 101 (52), 17958–17963.
- Tam, J.P., 1988. Synthetic peptide vaccine design: synthesis and properties of a high-density multiple antigenic peptide system. *Proc. Natl. Acad. Sci. U. S. A.* 85 (15), 5409–5413.
- Tam, J.P., Lu, Y.A., Yang, J.L., 2002. Antimicrobial dendrimeric peptides. *Eur. J. Biochem. / FEBS* 269 (3), 923–932.
- Teng, P.K., Eisenberg, D., 2009. Short protein segments can drive a non-fibrillizing protein into the amyloid state. *Protein Eng. Des. Sel. : PEDS* 22 (8), 531–536.
- Tenidis, K., Waldner, M., Bernhagen, J., Fischle, W., Bergmann, M., Weber, M., Merkle, M.L., Voelter, W., Brunner, H., Kapurniotu, A., 2000. Identification of a penta- and hexapeptide of islet amyloid polypeptide (IAPP) with amyloidogenic and cytotoxic properties. *J. Mol. Biol.* 295 (4), 1055–1071.
- Thompson, M.J., Sievers, S.A., Karanicolas, J., Ivanova, M.I., Baker, D., Eisenberg, D., 2006. The 3D profile method for identifying fibril-forming segments of proteins. *Proc. Natl. Acad. Sci. U. S. A.* 103 (11), 4074–4078.
- Uttamchandani, M., Yao, S.Q., 2008. Peptide microarrays: next generation biochips for detection, diagnostics and high-throughput screening. *Curr. Pharm. Des.* 14 (24), 2428–2438.
- Wang, X.J., Li, C.G., Chi, X.J., Wang, M., 2011. Characterisation and evaluation of antiviral recombinant peptides based on the heptad repeat regions of NDV and IBV fusion glycoproteins. *Virology* 416 (1–2), 65–74.
- Wild, C.T., Shugars, D.C., Greenwell, T.K., McDanal, C.B., Matthews, T.J., 1994. Peptides corresponding to a predictive alpha-helical domain of human immunodeficiency virus type 1 gp41 are potent inhibitors of virus infection. *Proc. Natl. Acad. Sci. U. S. A.* 91 (21), 9770–9774.
- von Bergen, M., Friedhoff, P., Biernat, J., Heberle, J., Mandelkow, E.-M., Mandelkow, E., 2000. Assembly of τ protein into Alzheimer paired helical filaments depends on a local sequence motif (306VQIVYK311) forming β structure. *Proc. Natl. Acad. Sci.* 97 (10), 5129–5134.
- Wouters, M.A., Curmi, P.M., 1995. An analysis of side chain interactions and pair correlations within antiparallel beta-sheets: the differences between backbone hydrogen-bonded and non-hydrogen-bonded residue pairs. *Proteins* 22 (2), 119–131.
- Xiao, X., Dimitrov, D.S., 2004. The SARS-CoV S glycoprotein. *Cell. Mol. Life Sci. : CMLS* 61 (19–20), 2428–2430.
- Xu, Y., Zhu, J., Liu, Y., Lou, Z., Yuan, F., Liu, Y., Cole, D.K., Ni, L., Su, N., Qin, L., Li, X., Bai, Z., Bell, J.I., Pang, H., Tien, P., Gao, G.F., Rao, Z., 2004. Characterization of the heptad repeat regions, HR1 and HR2, and design of a fusion core structure model of the spike protein from severe acute respiratory syndrome (SARS) coronavirus. *Biochemistry* 43 (44), 14064–14071.
- Yao, Q., Compans, R.W., 1996. Peptides corresponding to the heptad repeat sequence of human parainfluenza virus fusion protein are potent inhibitors of virus infection. *Virology* 223 (1), 103–112.
- Ying, W., Hao, Y., Zhang, Y., Peng, W., Qin, E., Cai, Y., Wei, K., Wang, J., Chang, G., Sun, W., Dai, S., Li, X., Zhu, Y., Li, J., Wu, S., Guo, L., Dai, J., Wang, J., Wan, P., Chen, T., Du, C., Li, D., Wan, J., Kuai, X., Li, W., Shi, R., Wei, H., Cao, C., Yu, M., Liu, H., Dong, F., Wang, D., Zhang, X., Qian, X., Zhu, Q., He, F., 2004. Proteomic analysis on structural proteins of severe acute respiratory syndrome coronavirus. *Proteomics* 4 (2), 492–504.
- Young, J.K., Li, D., Abramowitz, M.C., Morrison, T.G., 1999. Interaction of peptides with sequences from the Newcastle disease virus fusion protein heptad repeat regions. *J. Virol.* 73 (7), 5945–5956.
- Zhang, S.M., Jęjcic, A., Tam, J.P., Vahlne, A., 2015. Membrane-active sequences within gp41 Membrane Proximal External Region (MPER) modulate MPER-containing peptidyl fusion inhibitor activity and the biosynthesis of HIV-1 structural proteins. *PLoS One* 10 (7), e0134851.